Evaluation of the Bias in the Use of Clear-Sky Compared with All-Sky Observations of Monthly and Annual Daytime Land Surface Temperature

KEVIN GALLO[a] AND PRAVEENA KRISHNAN[b,c]

[a] *NOAA/NESDIS Center for Satellite Applications and Research, College Park, Maryland*
[b] *NOAA/Air Resources Laboratory Atmospheric Turbulence and Diffusion Division, Oak Ridge, Tennessee*
[c] *Oak Ridge Associated Universities, Oak Ridge, Tennessee*

(Manuscript received 17 November 2021, in final form 23 June 2022)

ABSTRACT: Satellite-derived observations of land surface temperature (LST) are being utilized in a growing number of land surface studies; however, these observations are generally obtained from optical sensors that exclude cloudy observations of the land surface. The impact of using only clear-sky observations of land surfaces on monthly and annual estimates of daytime LST over two U.S. Climate Reference Network (USCRN) sites was evaluated over five years with daily in situ LST observations available for all-sky (clear and cloudy) conditions. The in situ LST observations were obtained for the nominal daytime observations associated with the MODIS sensors on board the *Terra* and *Aqua* satellites and were identified as all-sky or clear-sky conditions by utilizing cloud information provided with the MODIS LST product. Both monthly/annual mean and monthly/annual maximum values of daytime LST were significantly different when only clear-sky values were utilized, in comparison with all-sky values. Monthly averaged differences between the mean clear- and all-sky daytime LST (dLST) values ranged from −0.1° ± 1.5°C for January to 5.6° ± 1.8°C for May. Annually averaged dLST values, over the five years of the study, were 2.58°C, and differences between the maximum values of clear- and all-sky daytime LST values were −1.03°C. Although significant differences between mean annual clear-sky and all-sky daytime LST values were more frequent than differences observed for the annual maximum daytime LST values, the results suggest that the exclusive use of either mean or maximum clear-sky daytime LST values is not advisable for applications in which the use of daytime all-sky LST values would be more applicable.

KEYWORDS: Land surface; Climatology; Cloud cover; Surface temperature; Climate records; Satellite observations

1. Introduction

Land surface temperature (LST), a key variable in the land surface–atmosphere exchange processes, has been identified as one of the most important environmental data records (WMO 2016; Popp et al. 2020) and is widely derived from satellite-based thermal infrared (IR) sensors (Dash et al. 2002; Li et al. 2013) because of its global coverage in various spatial and temporal resolutions.

Numerous studies have used satellite-derived observations of LST for ecological, biogeographical, climatological, and other land surface–related studies (e.g., Mildrexler et al. 2011; Tomlinson et al. 2011; Popp et al. 2020) and for indirect estimation of air temperature (Good 2016; Oyler et al. 2016; Pepin et al. 2016). Depending on the applications, these studies have utilized mean (e.g., Jaber and Abu-Allaban 2020; Jin and Dickinson 2010; Li et al. 2016; Yan et al. 2020) or maximum (Funk et al. 2019; Jiménez-Muñoz et al. 2013; Liu et al. 2021; Mildrexler et al. 2011) LST values over various time intervals. Previous studies suggest that the maximum temperature is more appropriate for assessment of large-scale thermal changes in climate systems than is mean daily averaged temperature (Pielke et al. 2007; Liu et al. 2021). Mildrexler et al. (2018) utilized maximum LST because of its potential to identify large-scale shifts in the biosphere and found that among several valuable uses, the maximum LST values provided valuable information related to ecosystem exposure to extreme temperatures. Funk et al. (2019) utilized maximum LST values in recognition that minimum LST values are more difficult to distinguish from clouds. As observed in these studies, there are potential issues of cloud interference with retrieval of satellite-derived LST products based on thermal IR data. Thus, these satellite-derived LST retrievals are limited to clear-sky conditions (e.g., Li et al. 2016) because of their inability to penetrate clouds and are not representative of all-sky (all weather) conditions (Wan 2008), which may lead to possible biases that need to be evaluated (Chen et al. 2017).

In recognition that there are differences between the LST values derived from clear-sky as compared with all-sky conditions there have been numerous methods proposed to estimate the cloudy-sky LST observations and create a complete record of daily LST observations. These proposed methods include the use of available ground-based LST observations, reanalysis products, statistical methods, gap filling, combination with satellite-based passive microwave measurements, or by reconstructing cloudy pixels by combining multiple satellite LST products (e.g., Chen et al. 2017; Duan et al. 2017; Li et al. 2018; Long et al. 2020; Martins et al. 2019; Prigent et al. 2016; Shiff et al. 2021; Wang et al. 2019; Zhang et al. 2015; Y. Zhang et al. 2020; Zhao and Duan 2020). Most of these methods still have low accuracies because of the use of clear-sky values in their methods, unidentified clouds, cloud detection errors, and an inability to completely remove the clouds containing pixels in satellite LST products (Ackerman et al. 1998, 2008; Williamson et al. 2013; Duan et al. 2017; Ermida

Corresponding author: Praveena Krishnan, praveena.krishnan@noaa.gov

DOI: 10.1175/JAMC-D-21-0240.1

For information regarding reuse of this content and general copyright information, consult the AMS Copyright Policy (www.ametsoc.org/PUBSReuseLicenses).

Brought to you by NOAA Central Library | Unauthenticated | Downloaded 07/19/23 03:29 PM UTC

et al. 2019; Bulgin et al. 2018). Thus, the use of spaceborne IR LST datasets in studies and applications will likely give results that are possibly biased toward the clear-sky conditions.

Despite its importance, the attempts to quantify the clear-sky bias of satellite-based LST, that is, the difference between clear-sky and all-sky LSTs, are scarce because of the absence of routinely available daily (all sky) satellite-derived LST. A few attempts include the estimation of clear-sky bias by using daily daytime and nighttime all-sky satellite passive microwave (MW) surface temperature measurements and cloud coverage information from MODIS LST product (Ermida et al. 2019) or by evaluating the relationship between the difference in 5-km monthly satellite LST and ground-based LST with clear-sky ratio (Chen et al. 2017). To avoid possible sources of uncertainties due to the differences in the LST retrieval techniques, sensors in different platforms, scale difference and heterogeneities, clear-sky bias has to be quantified using LST observations that use similar IR LST measurement techniques and platforms. In this context, it is important to quantify the clear-sky bias using similar LST observations especially during daytime (near solar noon) conditions, when the land surface experiences the higher end of the daily range of net radiation resulting in largest differences between clear and cloudy LSTs and also, due to the dependence of many land surface processes on daytime solar radiation and maximum temperatures (Gallo et al. 2011; Williamson et al. 2013).

This study was initiated, in the absence of routinely available daily (all sky) satellite-derived LST, to evaluate the bias in the exclusive use of clear-sky as compared with all-sky observations of monthly and annual daytime LST. The objective of this study was to use clear- and all-sky in situ observations of daytime LST to evaluate the differences introduced in computation and utilization of mean and maximum monthly daytime LST values when only clear-sky, as compared with all-sky, daytime LST observations are available. In this study, we have used continuous daytime LST data from two U.S. Climate Reference Network (USCRN) stations (Diamond et al. 2013) to compute both the clear and all-sky daytime monthly mean and maximum LST for the nominal observation times associated with the daytime *Terra* and *Aqua* MODIS sensors by using cloud information included with the MODIS daily daytime LST products to identify clear-sky conditions.

2. Method

The difference between clear-sky versus all-sky daytime LST was evaluated with continuous ground-based thermal infrared measurements of LST from two USCRN (https://www.ncdc.noaa.gov/crn; NOAA/NESDIS 2007; Diamond et al. 2013) stations because satellite IR sensors provide only clear-sky observations of LST. The two USCRN stations selected had exhibited a wide range in clear and cloudy observations in a previous study (Gallo et al. 2011). The USCRN station at Kingston 1W, Rhode Island (41.49°N, 71.54°W), exhibited a low number of clear days and high number of cloudy days while the station at Wolf Point 29ENE, Montana (48.31°N, 105.10°W), displayed relatively low number of cloudy days and high number of clear days. The LST observations at the USCRN sites were measured using Apogee Instruments, Inc., precision infrared temperature (IRT) sensors pointed at the ground surface (Krishnan et al. 2020). A default surface emissivity of 1.0 was used because the USCRN LST observations were made over grass vegetation ground cover with surface emissivity ~1.0. No other adjustments were made to the reported LST values at these USCRN sites to maintain consistency in LST measurements between the sites and to avoid any potential bias caused by additional corrections for reflected downwelling longwave radiation and surface emissivity (Gallo et al. 2011; Krishnan et al. 2015, 2020).

To identify the dates available for daytime clear-sky conditions of LST at the two USCRN sites for 2015–19, we have used the daytime quality control (QC) information associated with the land surface products retrieved from the MODIS sensors on board the *Terra* and *Aqua* satellites. The MODIS level 3 LST Collection-6 product suite (MOD11A1.006 products for *Terra* and MYD11A1.006 for *Aqua*) developed by Wan et al. (2002) and refined by Wan (2013) were retrieved with the Land Processes Distributed Active Archive Center (LP DAAC, https://lpdaac.usgs.gov/) application for extracting and exploring analysis ready samples (AppEEARS) tool (AppEEARS Team 2020). The daily daytime LST QC information (Wan 2013) derived from both *Terra* and *Aqua* MODIS sensors were retrieved for 2015–19 for the 1-km pixels containing each of the two USCRN stations and used to designate clear-sky periods over the USCRN sites. The MODIS LST values were not used in this analysis to estimate bias as the MODIS observed LST values were only available for clear-sky conditions. The MODIS QC and cloud mask information were used as mentioned above to partition the daytime observed in situ LST at the two USCRN sites into clear-sky and all-sky observations of LST.

The USCRN LST hourly averaged values (NOAA 2021) were retrieved for the nominal observation times associated with the daytime *Terra* and *Aqua* MODIS observations for the two USCRN stations. As recognized by Jin and Dickinson (2010) the daytime overpass time associated with the *Terra* MODIS LST products would be near 1030 local time; however, this time may vary by 90 min in low-latitude regions and as great as several hours in high-latitude regions. Similarly, the *Aqua* MODIS products would nominally be acquired at 1330 local time. The times of the clear-sky satellite-based LST observations during 2019 for the Kingston station ranged from 1012 to 1154 local time for the *Terra* MODIS observations and from 1206 to 1400 for the *Aqua* MODIS observations. The times of the clear-sky observations for the Wolf Point station ranged from 1012 to 1212 local time for the *Terra* observations and from 1154 to 1342 for the *Aqua* observations. The observation times were not provided for the cloudy-sky conditions when no LST values were available. For this analysis, the USCRN daily hourly average LST was retrieved for the hour starting at 1000 local standard time for the Kingston (1600 UTC) and Wolf Point (1800 UTC) USCRN locations for the *Terra* time of observations, and 1200 local standard time for the Kingston (1800 UTC) and Wolf Point (2000 UTC) *Aqua* observations.

The monthly daytime mean LST (LSTmean) values were computed from the USCRN LST data for the *Terra* and *Aqua*

Brought to you by NOAA Central Library | Unauthenticated | Downloaded 07/19/23 03:29 PM UTC

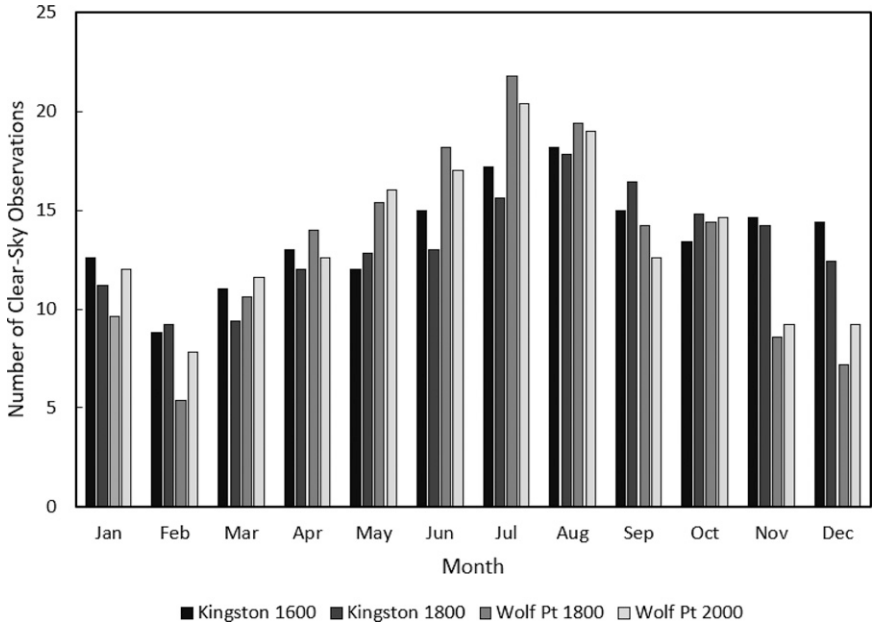

FIG. 1. Monthly average of the number of clear-sky observations over Kingston and Wolf Point for the two observation times (UTC) associated with each station during 2015–19.

overpass times associated with each station based on the average of 1) all available (all sky) USCRN LST values and 2) the USCRN LST values for the clear-sky conditions (as designated by the MODIS QC and cloud information). Similarly, the monthly maximum LST (LSTmax) values were computed for clear-sky and all-sky conditions.

The differences in the monthly mean (dLST) and maximum (dLSTmax) daytime LST values derived from the clear-sky and all-sky USCRN in situ observations were computed as

$$\text{dLST} = \text{LSTmean(clear sky)} - \text{LSTmean(all sky)}, \quad (1)$$

and

$$\text{dLSTmax} = \text{LSTmax(clear sky)} - \text{LSTmax(all sky)}. \quad (2)$$

The differences in the clear- and all-sky number of observations, and values of the observations, were evaluated for the five years, two stations, and two observation times included in the analysis. Because of the differences in the number of available observations for the clear-sky and all-sky LST values, the monthly daytime LSTmean values were evaluated with the nonparametric Wilcoxon rank sums test (SAS 2018a). The annual daytime dLST and dLSTmax values were evaluated, based on the available monthly values, with *t*-test (SAS 2018b) and ANOVA analyses (SAS 2018c).

3. Results

a. *Number of available observations*

The number of clear-sky observations varied considerably over the five years included in the analysis as well as within each of the years. The monthly number of clear-sky observations averaged over the five years of the study was highly variable among the individual months (Fig. 1). The number of clear-sky observations varied from a minimum of two observations for Wolf Point (1800 UTC) during February 2015 to a maximum of 26 observations for Wolf Point (1800 UTC) during July 2018. In general, the months of November–March exhibited the lowest number of clear-sky observations.

The percentage of clear-sky observations per year (Fig. 2) were generally one-half (or less) of the total possible (all sky) observations over all five years for both locations and observation times. The ratio of annual clear-sky to all-sky observations varied from a minimum of 40.5% for the Wolf Point 1800 UTC observations in 2019 to a maximum of 51.6% for the Kingston 1800 UTC observations in 2016. The overall mean number of clear-sky observations (all years, for both USCRN locations and observation times) was 44.1% of the possible number of observations. The number of clear-sky observations per year over these two sites are in close agreement with the regional and global scale estimates of average percentage (<50%) of daytime clear-sky pixels derived from satellite-based observations (Wan et al. 2004; Duan et al. 2017; Z. Zhang et al. 2020).

b. *Impact of available observations on mean and maximum LST*

The impact of the number of daytime observations associated with the clear-sky, as compared with all-sky, conditions on mean and maximum LST was demonstrated through the review of a single month (March 2019) and subsequent year (2019) for the observations at the Kingston location. This location, month, and year were selected on the basis of initial results that suggested further investigation of the details related to these results was warranted (Table 1).

Brought to you by NOAA Central Library | Unauthenticated | Downloaded 07/19/23 03:29 PM UTC

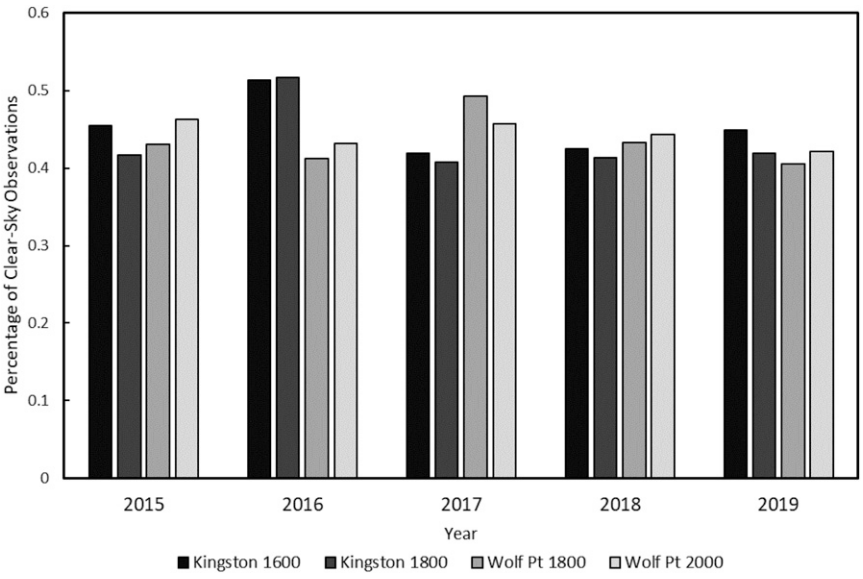

FIG. 2. Percentage of annual clear-sky observations over Kingston and Wolf Point for the two observation times (UTC) associated with each station during 2015–19.

The daily and mean monthly values of clear- and all-sky values of in situ LST, for the 1600 (Fig. 3a) and 1800 UTC (Fig. 3b) observations for Kingston, are displayed for March 2019. There were 14 clear-sky observations this month at the 1600 observation time (Fig. 3a). The clear-sky mean LST (7.28°C) at this time was nearly identical to the all-sky value (7.26°C). The maximum values, however, differed considerably with the maximum clear-sky LST value of 15.5°C observed on 24 March 2019 (Fig. 3a) while the maximum all-sky observed LST value of 25.2°C was observed on 30 March (a date identified as cloudy by MODIS information). The 1800 UTC observations (Fig. 3b) included only 10 clear-sky observations. The results for the 1800 UTC observations included differences of 5.09°C between the mean values of the clear-sky observations (14.1°C) and the all-sky observations (9.01°C). The maximum clear-sky and all-sky LST values (20.0°C) were the same, as they were both observed on the same date (24 March 2019).

TABLE 1. The monthly and annual dLST and dLSTmax values for the 1600 and 1800 UTC observations at Kingston in 2019, with significance of the clear-sky and all-sky monthly (available only for dLST) and annual differences indicated. Note that single and double asterisks denote significance at $p \leq 0.05$ and $p \leq 0.01$, respectively.

	dLST		dLSTmax	
Month	1600	1800	1600	1800
Jan	−1.67	−1.16	−6.70	0.00
Feb	0.16	2.88	−0.70	0.00
Mar	0.02	5.09*	−9.70	0.00
Apr	2.70	3.71*	−2.60	−0.40
May	5.43*	5.36*	0.00	0.00
Jun	2.29*	2.01	0.00	0.00
Jul	1.86*	1.49	0.00	0.00
Aug	1.22	1.33	0.00	0.00
Sep	1.34	1.00	0.00	0.00
Oct	1.36	1.71*	−1.00	−9.00
Nov	−0.66	0.62	−2.70	−2.30
Dec	−1.11	−0.45	−6.60	−1.30
Mean	1.08	1.96**	−2.50*	−1.08

The results of the mean and maximum March 2019 observations of LST for Kingston (Fig. 3) are displayed with similar observations for all months during 2019 (Fig. 4). The nearly identical March monthly mean values for clear- and all-sky LST observations (Fig. 3a) is depicted in the displayed monthly values for Kington at 1600 UTC (Fig. 4a). The difference in maximum values of clear- and all-sky LST observations displayed in Fig. 3a is displayed in Fig. 4b. In general, the mean monthly LST values during 2019 are greater for the clear-sky observations, at both 1600 (Fig. 4a) and 1800 UTC (Fig. 4c) than for the all-sky observations, during the spring–autumn months. During this interval, the land surface under clear conditions would be expected to be warmer than the all-sky observations (which would include observations under cloudy conditions). During the winter months, however, the cloudy conditions included in the all-sky observations would provide an insulating effect, which resulted in the all-sky observations being equal to, or warmer than, the clear-sky observations. Similar results were observed for the Wolf Point location.

The monthly maximum all-sky LST was greater or equal to the clear-sky maximum LST for both the 1600 (Fig. 4b) and 1800 UTC (Fig. 4d) observations for all months. This would be expected because every clear-sky LST observation would be included in the all-sky observations. Any differences in the observed maximum temperatures between the clear-sky and all-sky monthly values would be due to a USCRN in situ observation being utilized for the all-sky observation, however, not

Brought to you by NOAA Central Library | Unauthenticated | Downloaded 07/19/23 03:29 PM UTC

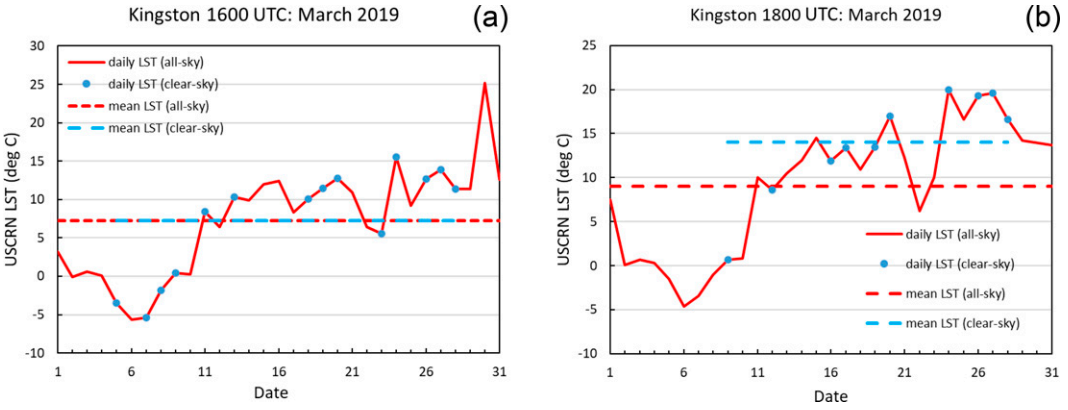

FIG. 3. Daytime daily and monthly mean clear-sky and all-sky USCRN in situ LST (°C) values for Kingston at (a) 1600 and (b) 1800 UTC observation times for March 2019.

included as a clear-sky observation as a result of the MODIS cloud information that designated the observation as cloudy.

c. *Differences in clear-sky and all-sky monthly and annual mean and maximum LST values*

The daytime monthly mean and maximum values for the clear- and all-sky observations were used in Eqs. (1) and (2) to derive the differences in the clear- and all-sky monthly mean (dLST) and maximum (dLSTmax) observed LST. The dLST and dLSTmax values for each of the months for Kingston at the 1600 and 1800 UTC observation times during 2019 are displayed in Table 1 for comparisons with the results in Fig. 4 and indication of the significant values. The monthly mean clear-sky observations of LST are generally greater than the all-sky observations (Figs. 4a,c) such that the resulting dLST values [Eq. (1)] are generally positive for both observation times, which resulted in a mean annual dLST of 1.08° and 1.96°C for the 1600 and 1800 UTC observation times, respectively.

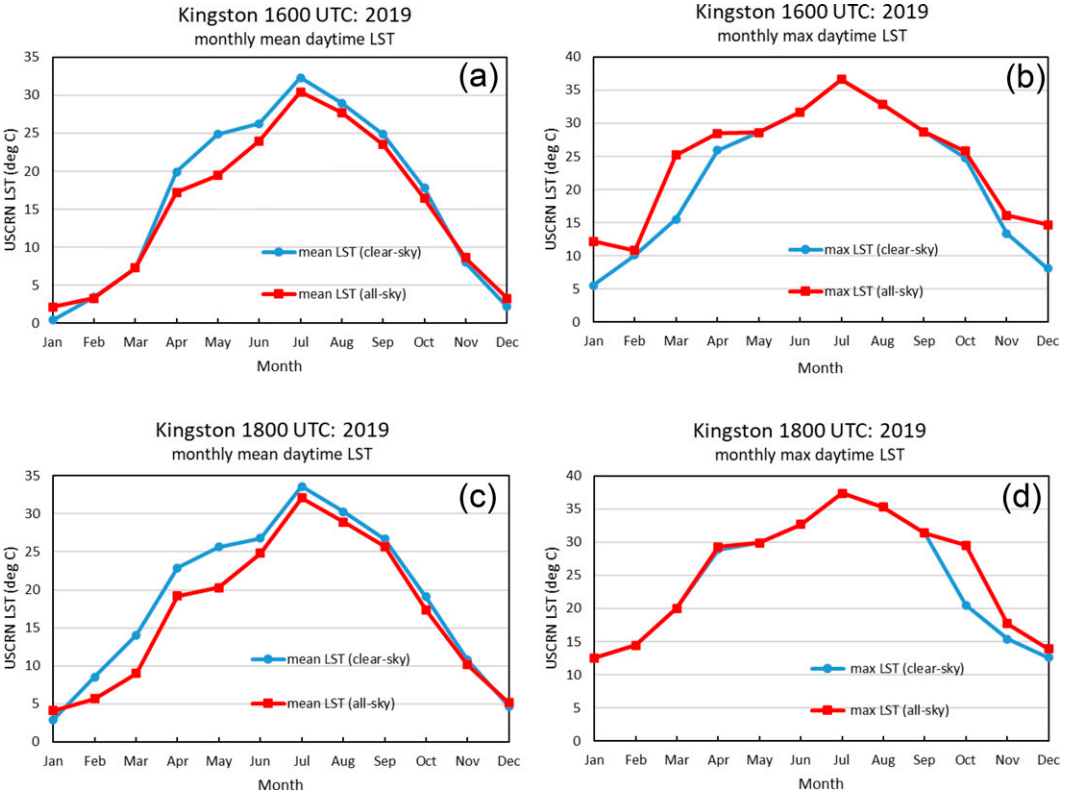

FIG. 4. Daytime monthly (left) mean and (right) maximum clear-sky and all-sky USCRN in situ LST values (°C) for Kingston at (a),(b) 1600 and (c),(d) 1800 UTC observation times for 2019.

Brought to you by NOAA Central Library | Unauthenticated | Downloaded 07/19/23 03:29 PM UTC

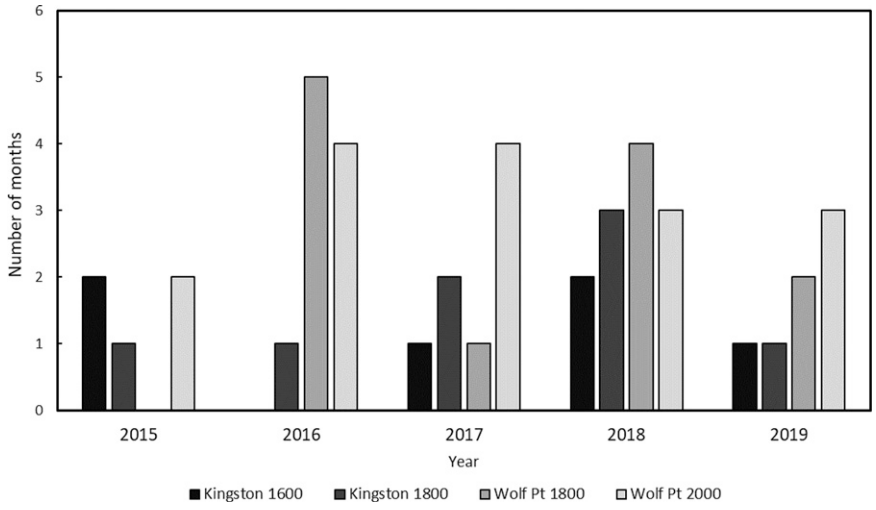

FIG. 5. Number of months with significant differences ($p \leq 0.05$) in dLST for each year at the Kingston and Wolf Point stations.

From the analysis of the clear-sky and all-sky LST values observed at Kingston for the individual months (Table 1), three and four months displayed significant differences ($p \leq 0.05$) in dLST at the 1600 and 1800 UTC observation times, respectively. Significant differences ($p \leq 0.05$) in dLST on a monthly basis for both stations (Fig. 5) ranged from a minimum of zero months with significant differences (Wolf Point, 1800 UTC observation for 2015; Kingston, 1600 UTC observations for 2016) to a maximum of five months (Wolf Point, 1800 UTC observation for 2016).

An analysis of the combined results of both stations (Fig. 6) indicated that the winter months exhibited little or no differences in the LST values while 85% of the values observed during May were significantly different. Similar to the 2019 results for Kington displayed in Table 1, the spring months of April and May display some of the larger dLST values. Mean monthly dLST values ranged from −0.1° ± 1.5°C during January to 5.6° ± 1.8°C during May.

The clear-sky maximum daytime LST values observed at Kingston (Figs. 4b,d), are equal or less than the all-sky LST values such that the resulting dLSTmax values [Eq. (2)] are zero or negative, which resulted in a mean annual dLSTmax (Table 1) of −2.50° and −1.08°C for the 1600 and 1800 UTC observation times, respectively. The dLST values were significant at the $p \leq 0.01$ level for the 1800 UTC observations and the dLSTmax values were significant at the $p \leq 0.05$ level for the 1600 UTC observations.

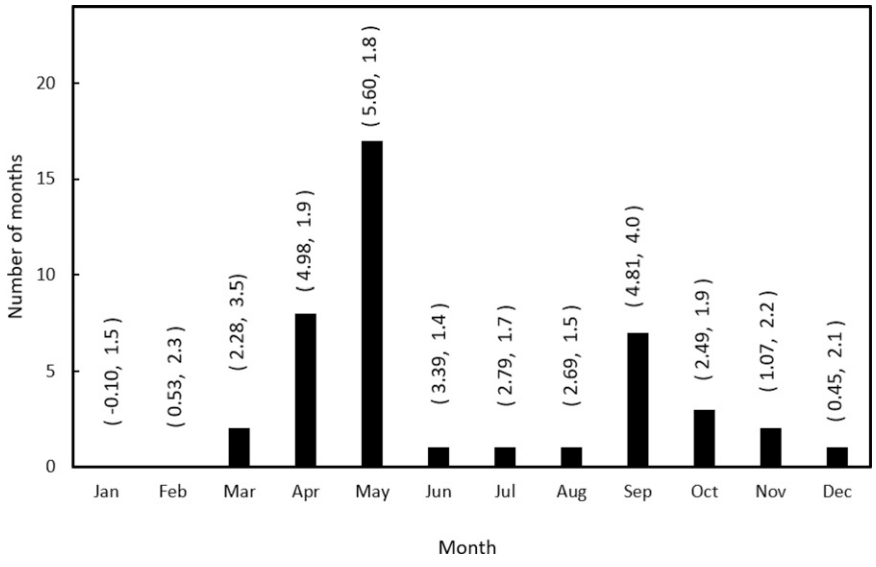

FIG. 6. Number of months with significant differences ($p \leq 0.05$) in dLST for each month for the two locations, two observation times, and five years ($n = 20$ month^{-1}). The values in parentheses are the mean and standard deviation values (°C) of dLST associated with each month.

Brought to you by NOAA Central Library | Unauthenticated | Downloaded 07/19/23 03:29 PM UTC

TABLE 2. Kingston and Wolf Point annual dLST and dLSTmax values for 2015–19, with significance of clear-sky and all-sky differences indicated. All times are UTC. Note that single and double asterisks denote significance at $p \leq 0.05$ and $p \leq 0.01$, respectively.

	Kingston				Wolf Point			
	dLST		dLSTmax		dLST		dLSTmax	
Year	1600	1800	1600	1800	1800	2000	1800	2000
2015	0.54	1.13	−1.27*	−1.34*	2.80**	3.68**	−1.11	−0.29
2016	1.17*	1.96**	−1.01*	−1.23*	4.12**	4.82**	−0.25	−0.83
2017	1.33	2.71**	−1.25	−1.00	3.19**	4.80**	−0.16	−0.38
2018	1.46	2.23**	−1.46	−0.78	3.49*	3.80*	−0.92	−0.83*
2019	1.08	1.96**	−2.50*	−1.08	2.30*	3.07**	−1.57	−1.30

When examined over the five years of the study (Table 2) the annual dLST values were significant ($p \leq 0.05$) for 5 of the 10 combinations of observation times and years for Kingston and all of the Wolf Point observation years. The dLSTmax values, similar to the dLST, were significant for 5 of the 10 observation years for the Kingston location. However, unlike the Kingston results, there was only one (of 10) observation years (2000 UTC for 2018) in which the dLSTmax values for clear- and all-sky conditions were significantly different at Wolf Point.

When the annual differences in observed results of the two locations (Table 2) are combined there were significant differences ($p \leq 0.05$) observed in the annual clear-sky and all-sky mean LST (dLST) values for 75% of the 20 observation years while significant differences in the clear-sky and all-sky maximum LST (dLSTmax) values were observed for only 6 of the 20 observation years. Annual averaged differences between mean clear- and all-sky daytime LST values were 2.58°C while differences between the maximum values of clear- and all-sky daytime LST values were −1.03°C.

An analysis of variance associated with the results indicated that within this limited study both the observation station location and observation time were statistically significant factors ($p \leq 0.05$) associated with the differences observed in clear-sky and all-sky mean monthly temperatures. The analysis of the differences in clear- and all-sky monthly maximum temperatures indicated that station location was a statistically significant factor ($p \leq 0.10$) associated with the observed differences.

4. Discussion

This study evaluates the effect of using clear-sky daytime LST instead of all-sky (all-weather) daytime LST observations on the monthly mean and maximum LST values and its effect on annual values. The clear-sky bias is estimated as the difference between clear-sky LST and all-sky LST. Clear-sky bias was estimated from daytime hourly in situ (surface based) observations of LST measured with infrared temperature sensors with accuracy $< \pm 0.5$°C (Krishnan et al. 2020) at the two USCRN stations. The in situ LST observations corresponded to the nominal daytime *Terra/Aqua* overpass times over the two locations to match the available MODIS cloud information with the in situ LST observations at the stations. It should be noted that the daytime monthly mean LST in this study is different from the true monthly mean temperature estimated using the continuous LST measurements covering all diurnal cycles in a month divided by the measurement period (Zeng and Wang 2012). The QC and cloud information associated with the MODIS LST products are used to identify the clear-sky periods. These periods correspond to daytime conditions when land experiences the greatest daily net radiation. This is particularly true for *Aqua* overpass time when the clear-sky LST would be expected to be near the maximum value for the land surface (Chen et al. 2017). Daytime monthly maximum LST was also included in this study, using daily maximum temperatures observed during clear-sky conditions. The use of daytime LST values is important because many processes are dependent on daylight and maximum temperature (Williamson et al. 2013). Monthly maximum LST is widely used as the official climate record of monthly temperature and is used in studies focusing on the regional and global climate change (Trenberth et al. 2007) and also for the spatial–temporal validation of large-scale land surface models (Koch et al. 2016).

However, the attempts to quantify the clear-sky bias in satellite-based IR LST and assessment of the impact of relying only on clear-sky data in the above studies are still scarce. Recently Ermida et al. (2019) assessed the clear-sky bias of satellite MW LST at a global scale by utilizing Advanced Microwave Scanning Radiometer for Earth Observing System (AMSR-E) passive MW-based LST estimates. The MW measurements were used as a surrogate for IR LST. Cloud coverage information provided from MODIS was used to identify clear-sky and all-sky conditions and a daytime bias of 2–8 K was observed between the clear-sky and all-sky LST over the midlatitudes. However, uncertainties still exist in the estimate of clear-sky bias by this method because of potential differences in the LST retrieval by IR and MW sensors, that is, skin temperature observed by IR sensors as compared with surface–subsoil temperatures observed by MW sensors. The MW LST bias with respect to LST by IR sensors alone can vary up to <4 K (Ermida et al. 2017). In contrast, Chen et al. (2017) reported a lack of any significant bias due to cloud contamination on monthly LST based on the relationship between the difference between 5-km monthly MODIS LST (MOD11C3) and in situ LST over 156 sites. The major sources of uncertainties in this analysis included the difference in the spectral bands used by the MODIS and in situ sensors, and the scale difference between the spatial footprint of ground-based point measurements and the 5-km MODIS LST product satellite platforms. Additionally, additive errors in LST and emissivity due to inhomogeneity, as evident from large RMSE between in situ LSTs and satellite LSTs (Guillevic et al. 2012; Krishnan et al. 2015, 2020), cannot be neglected. However, Chen et al. (2017) found that the monthly mean values from MODIS day and night clear-sky observations were slightly higher than monthly all-sky in situ LST. This result suggests the importance of evaluation of clear-sky bias using LST measurements made with consistent sensors with high accuracy

Brought to you by NOAA Central Library | Unauthenticated | Downloaded 07/19/23 03:29 PM UTC

and similar field of view. To the best of our knowledge, the present study represents a first attempt to assess and quantify clear-sky bias of monthly daytime LST and its seasonal variation utilizing in situ surface-based observations that are coincident in time with the observed satellite sensor LST.

The two sites included in this study were selected based on the number of clear and cloudy observations reported in Gallo et al. (2011). The USCRN station at Kingston exhibited a low number of clear days and a high number of cloudy days whereas the Wolf Point 29ENE station exhibited a relatively low number of cloudy days and high number of clear days representing the range of clear-sky days. During the 5-yr period from 2015 to 2019 yearly daytime clear-sky observations at these sites varied from 40% to 52% (from 118 to 189 days), agreeing with previous reports (<50%) on regional and global estimates of average clear-sky grids derived from satellite-based observations (Wan et al. 2004; Duan et al. 2017; Z. Zhang et al. 2020). Even though the percentage of clear-sky observations at these sites are similar to the global average, extreme cloudy or clear conditions can occur in other global environments. Monsoon regions or low latitudes that experience persistent cloud cover present the low extreme of clear-sky days, while the number of clear-sky days can vary up to 340 days yr^{-1} in arid regions across the globe (Z. Zhang et al. 2020) that can result in a low clear-sky bias in arid regions (Ermida et al. 2019).

The number of clear-sky observations at the USCRN stations included in this study follows a seasonal pattern that appears to be controlled by the seasonal variations of solar radiation at these sites with peak values in summer. Annual clear-sky observations exhibited interannual variations with a maximum number of clear-sky days exceeding 180 days at Kingston in 2016, but with no trend. In this study, we have used MODIS cloud information, over the 1-km pixel that includes the in situ LST observation stations, to detect cloud presence over the site. Previous studies indicated that the MODIS cloud information results agree with ground-based active sensors up to 85% (Ackerman et al. 2008) and unidentified clouds in MODIS LST product can vary between 13% and 17% (Williamson et al. 2013).

Within this study the impact of the use of clear-sky as compared with all-sky LST was most evident in the results observed from daytime monthly mean values rather than monthly maximum values. The clear-sky bias within monthly mean daytime LST was generally positive at both sites as expected due to the increased contribution of solar radiation (Schwingshackl et al. 2018) under clear-sky conditions leading to higher LST especially from spring to autumn. The highest clear-sky bias (5.6°C in May; Fig. 6) occurred mostly during the spring followed by autumn months (4.81°C in September) when changes in snow cover, soil water content and onset or senescence of vegetation are greatest due to the seasonal climate conditions at these locations. This result suggests that the magnitude of clear-sky bias can be influenced by the land surface radiative properties during the transition periods while the greater number of clear-sky days in summer resulted in low magnitudes of clear-sky bias. This pattern agrees with the monthly variation of bias estimated using MW LST by Ermida et al. (2019) over North America. The magnitude and distribution of clear-sky bias can vary on regional and global scales as the distribution of the types of clouds, the number of clear-sky days per year, and its seasonal variation depend on the geographical location of the site and the prevailing environmental conditions (Zhang et al. 2015; Z. Zhang et al. 2020).

While this study was limited to an assessment of clear-sky bias over two sites in North America, the results clearly demonstrated the impact of clear-sky versus all-sky LST observations on the monthly and annual mean day time temperatures. The use of annual maximum LST does minimize the influence of synoptic and seasonal variability and can provide information associated with extreme climatic events and significant land-cover changes. However, the impact of the use of maximum LST bias on applications that require LST observations, especially climate studies, is still uncertain. LST is often assimilated into land surface models for short and medium range forecasting to improve land–atmosphere exchange simulations (Qin et al. 2007; Reichle et al. 2010; Rodell et al. 2004) and for the indirect estimation of near-surface air temperature, but the effect of using clear-sky versus all-sky observations in these studies yet to be investigated. However, studies of the impact of all-sky solar irradiance on assimilation experiments showed that they provided a higher degree of improvement when compared with only clear-sky observations (Okamoto et al. 2019). The use of satellite-derived LST to examine the long-term LST trends at regional and global scales and their drivers (Abera et al. 2020; Liu et al. 2021; Yan et al. 2020), applications relevant to climate change monitoring, or assessing impact of land-cover changes (Li et al. 2016), suggest that a better understanding of the bias resulting from the use of clear-sky as compared with all-sky LST observations could potentially lead to more accurate assessment of trends and lead to more definitive conclusions.

5. Conclusions

From an analysis of USCRN station hourly in situ observations of daytime LST coupled with MODIS-designated clear-sky and all-sky conditions, the results of this study indicate that both monthly/annual mean and monthly/annual maximum values of daytime LST can differ significantly when only clear-sky (as compared with all-sky) values of LST are utilized. Monthly averaged differences between the mean clear- and all-sky daytime LST (dLST) values varied considerably by month. The winter months exhibited little or no differences in the dLST values; however, 85% of the monthly dLST values observed for the month of May were significantly different. Mean monthly dLST ranged from $-0.1° \pm 1.5$°C for January to $5.6° \pm 1.8$°C for May. Annually averaged dLST values, over the five years of the study, were 2.58°C while differences between the maximum values of clear- and all-sky daytime LST values were −1.03°C. While significant differences between the mean annual clear-sky and all-sky LST values were more frequent than the differences observed for the annual maximum LST values, the results suggest that the

Brought to you by NOAA Central Library | Unauthenticated | Downloaded 07/19/23 03:29 PM UTC

exclusive use of either mean or maximum clear-sky LST values is not advisable for applications in which the use of all-sky LST values would be more applicable.

This study was based the LST observations at times associated with the daytime overpass times of the *Terra* and *Aqua* MODIS sensors, but the results of this analysis would also be applicable to other satellite-derived LST observations acquired with similar orbital characteristics. Thus, the results should be applicable to the LST observations acquired with the *Suomi-NPP* and *NOAA-20* [*Joint Polar Satellite System-1* (*JPSS-1*)] VIIRS sensors that have similar observation times (nominal 1330 local overpass times) to the *Aqua* MODIS observation times evaluated in this analysis. The results should also be applicable to the daytime observations acquired by geostationary satellite-based sensors (e.g., GOES-R series and others) that permit consistent (day and night) observations.

Acknowledgments. This research was partially funded by NOAA's U.S. Climate Reference Network program and the Center for Satellite Applications and Research (STAR) GOES-R and JPSS programs. The scientific results and conclusions, as well as any views or opinions expressed herein, are those of the authors and do not necessarily reflect those of NOAA or the U.S. Department of Commerce.

Data availability statement. The USCRN data used in this study are available as described online (https://www.ncei.noaa.gov/pub/data/uscrn/products/hourly02/README.txt; accessed 17 November 2021), and the MODIS data utilized are also available online (https://lpdaacsvc.cr.usgs.gov/appeears; accessed 17 November 2021).

REFERENCES

Abera, T. A., J. Heiskanen, E. E. Maeda, and P. K. E. Pellikka, 2020: Land surface temperature trend and its drivers in East Africa. *J. Geophys. Res. Atmos.*, **125**, e2020JD033446, https://doi.org/10.1029/2020JD033446.

Ackerman, S. A., K. I. Strabala, W. P. Menzel, R. A. Frey, C. C. Moeller, and L. E. Gumley, 1998: Discriminating clear sky from clouds with MODIS. *J. Geophys. Res.*, **103**, 32 141–32 157, https://doi.org/10.1029/1998JD200032.

——, R. E. Holz, R. Frey, E. W. Eloranta, B. C. Maddux, and M. J. McGill, 2008: Cloud detection with MODIS: Part II. Validation. *J. Atmos. Oceanic Technol.*, **25**, 1073–1086, https://doi.org/10.1175/2007JTECHA1053.1.

AppEEARS Team, 2020: Application for extracting and exploring analysis ready samples (AppEEARS), version. 2.30. NASA EOSDIS LP DAAC, USGS/EROS Center, accessed 17 November 2021, https://lpdaacsvc.cr.usgs.gov/appeears.

Bulgin, C. E., C. J. Merchant, D. Ghent, L. Klüser, T. Popp, C. Poulsen, and L. Sogacheva, 2018: Quantifying uncertainty in satellite-retrieved land surface temperature from cloud detection errors. *Remote Sens.*, **10**, 616, https://doi.org/10.3390/rs10040616.

Chen, X., Z. Su, Y. Ma, J. Cleverly, and M. Liddell, 2017: An accurate estimate of monthly mean land surface temperatures from MODIS clear-sky retrievals. *J. Hydrometeor.*, **18**, 2827–2847, https://doi.org/10.1175/JHM-D-17-0009.1.

Dash, P., F.-M. Göttsche, F.-S. Olesen, and H. Fischer, 2002: Land surface temperature and emissivity estimation from passive sensor data: Theory and practice-current trends. *Int. J. Remote Sens.*, **23**, 2563–2594, https://doi.org/10.1080/01431160110115041.

Diamond, H. J., and Coauthors, 2013: U.S. Climate Reference Network after one decade of operations: Status and assessment. *Bull. Amer. Meteor. Soc.*, **94**, 485–498, https://doi.org/10.1175/BAMS-D-12-00170.1.

Duan, S.-B., Z.-L. Li, and P. Leng, 2017: A framework for the retrieval of all-weather land surface temperature at a high spatial resolution from polar-orbiting thermal infrared and passive microwave data. *Remote Sens. Environ.*, **195**, 107–117, https://doi.org/10.1016/j.rse.2017.04.008.

Ermida, S. L., C. Jiménez, C. Prigent, I. F. Trigo, and C. C. DaCamara, 2017: Inversion of AMSR-E observations for land surface temperature estimation: 2. Global comparison with infrared satellite temperature. *J. Geophys. Res. Atmos.*, **122**, 3348–3360, https://doi.org/10.1002/2016JD026148.

——, I. F. Trigo, C. C. DaCamara, C. Jiménez, and C. Prigent, 2019: Quantifying the clear-sky bias of satellite land surface temperature using microwave-based estimates. *J. Geophys. Res. Atmos.*, **124**, 844–857, https://doi.org/10.1029/2018JD029354.

Funk, C., and Coauthors, 2019: A high-resolution 1983–2016 T_{max} climate data record based on infrared temperatures and stations by the Climate Hazard Center. *J. Climate*, **32**, 5639–5658, https://doi.org/10.1175/JCLI-D-18-0698.1.

Gallo, K., R. Hale, D. Tarpley, and Y. Yu, 2011: Evaluation of the relationship between air and land surface temperature under clear-and cloudy-sky conditions. *J. Appl. Meteor. Climatol.*, **50**, 767–775, https://doi.org/10.1175/2010JAMC2460.1.

Good, E. J., 2016: An in situ-based analysis of the relationship between land surface "skin" and screen-level air temperatures. *J. Geophys. Res. Atmos.*, **121**, 8801–8819, https://doi.org/10.1002/2016JD025318.

Guillevic, P. C., J. L. Privette, B. Coudert, M. A. Palecki, J. Demarty, C. Ottle, and J. A. Augustine, 2012: Land surface temperature product validation using NOAA's surface climate observation networks—Scaling methodology for the visible infrared imager radiometer suite (VIIRS). *Remote Sens. Environ.*, **124**, 282–298, https://doi.org/10.1016/j.rse.2012.05.004.

Jaber, S. M., and M. M. Abu-Allaban, 2020: MODIS-based land surface temperature for climate variability and change research: The tale of a typical semi-arid to arid environment. *Eur. J. Remote Sens.*, **53**, 81–90, https://doi.org/10.1080/22797254.2020.1735264.

Jiménez-Muñoz, J. C., J. A. Sobrino, C. Mattar, and Y. Malhi, 2013: Spatial and temporal patterns of the recent warming of the Amazon forest. *J. Geophys. Res. Atmos.*, **118**, 5204–5215, https://doi.org/10.1002/jgrd.50456.

Jin, M., and R. E. Dickinson, 2010: Land surface skin temperature climatology: Benefitting from the strengths of satellite observations. *Environ. Res. Lett.*, **5**, 044004, https://doi.org/10.1088/1748-9326/5/4/044004.

Koch, J., A. Siemann, S. Stisen, and J. Sheffield, 2016: Spatial validation of large-scale land surface models against monthly land surface temperature patterns using innovative performance metrics. *J. Geophys. Res. Atmos.*, **121**, 5430–5452, https://doi.org/10.1002/2015JD024482.

Krishnan, P., J. Kochendorfer, E. J. Dumas, P. C. Guillevic, C. B. Baker, T. P. Meyers, and B. Martos, 2015: Comparison of in-situ, aircraft, and satellite land surface temperature measurements over a NOAA Climate Reference Network site.

Brought to you by NOAA Central Library | Unauthenticated | Downloaded 07/19/23 03:29 PM UTC

Remote Sens. Environ., **165**, 249–264, https://doi.org/10.1016/j.rse.2015.05.011.

——, T. P. Meyers, S. J. Hook, M. Heuer, D. Senn, and E. J. Dumas, 2020: Intercomparison of in situ sensors for ground-based land surface temperature measurements. *Sensors*, **20**, 5268, https://doi.org/10.3390/s20185268.

Li, X., Y. Zhou, G. R. Asrar, and Z. Zhu, 2018: Creating a seamless 1 km resolution daily land surface temperature dataset for urban and surrounding areas in the conterminous United States. *Remote Sens. Environ.*, **206**, 84–97, https://doi.org/10.1016/j.rse.2017.12.010.

Li, Y., and Coauthors, 2016: Potential and actual impacts of deforestation and afforestation on land surface temperature. *J. Geophys. Res. Atmos.*, **121**, 14 372–314 386, https://doi.org/10.1002/2016JD024969.

Li, Z.-L., B.-H. Tang, H. Wu, H. Ren, G. Yan, Z. Wan, I. F. Trigo, and J. A. Sobrino, 2013: Satellite-derived land surface temperature: Current status and perspectives. *Remote Sens. Environ.*, **131**, 14–37, https://doi.org/10.1016/j.rse.2012.12.008.

Liu, J., D. F. T. Hagan, and Y. Liu, 2021: Global land surface temperature change (2003–2017) and its relationship with climate drivers: AIRS, MODIS, and ERA5-land based analysis. *Remote Sens.*, **13**, 44, https://doi.org/10.3390/rs13010044.

Long, D., and Coauthors, 2020: Generation of MODIS-like land surface temperatures under all-weather conditions based on a data fusion approach. *Remote Sens. Environ.*, **246**, 111863, https://doi.org/10.1016/j.rse.2020.111863.

Martins, J. P. A., and Coauthors, 2019: An all-weather land surface temperature product based on MSG/SEVIRI observations. *Remote Sens.*, **11**, 3044, https://doi.org/10.3390/rs11243044.

Mildrexler, D. J., M. Zhao, and S. W. Running, 2011: A global comparison between station air temperatures and MODIS land surface temperatures reveals the cooling role of forests. *J. Geophys. Res.*, **116**, G03025, https://doi.org/10.1029/2010JG001486.

——, ——, W. B. Cohen, S. W. Running, X. P. Song, and M. O. Jones, 2018: Thermal anomalies detect critical global land surface changes. *J. Appl. Meteor. Climatol.*, **57**, 391–411, https://doi.org/10.1175/JAMC-D-17-0093.1.

NOAA, 2021: USCRN/USRCRN Hourly Files. Accessed 17 November 2021, https://www.ncei.noaa.gov/pub/data/uscrn/products/hourly02/README.txt.

NOAA/NESDIS, 2007: United States Climate Reference Network (USCRN) functional requirements document. NOAA Doc. NOAA-CRN/OSD-2003-0009R1UD0, 15 pp., https://www.ncei.noaa.gov/pub/data/uscrn/documentation/program/X040_d0.pdf.

Okamoto, K., Y. Sawada, and M. Kunii, 2019: Comparison of assimilating all-sky and clear-sky infrared radiances from *Himawari-8* in a mesoscale system. *Quart. J. Roy. Meteor. Soc.*, **145**, 745–766, https://doi.org/10.1002/qj.3463.

Oyler, J. W., S. Z. Dobrowski, Z. A. Holden, and S. W. Running, 2016: Remotely sensed land skin temperature as a spatial predictor of air temperature across the conterminous United States. *J. Appl. Meteor. Climatol.*, **55** 1441–1457, https://doi.org/10.1175/JAMC-D-15-0276.1.

Pepin, N., E. E. Maeda, and R. Williams, 2016: Use of remotely sensed land surface temperature as a proxy for air temperatures at high elevations: Findings from a 5000 m elevational transect across Kilimanjaro. *J. Geophys. Res. Atmos.*, **121**, 9998–10 015, https://doi.org/10.1002/2016JD025497.

Pielke, R. A., Sr., and Coauthors, 2007: Unresolved issues with the assessment of multidecadal global land surface temperature trends. *J. Geophys. Res.*, **112**, D24S08, https://doi.org/10.1029/2006JD008229.

Popp, T., and Coauthors, 2020: Consistency of satellite climate data records for Earth system monitoring. *Bull. Amer. Meteor. Soc.*, **101**, E1948–E1971, https://doi.org/10.1175/BAMS-D-19-0127.1.

Prigent, C., C. Jimenez, and F. Aires, 2016: Toward "all weather," long record, and real-time land surface temperature retrievals from microwave satellite observations. *J. Geophys. Res. Atmos.*, **121**, 5699–5717, https://doi.org/10.1002/2015JD024402.

Qin, J., S. Liang, R. Liu, H. Zhang, and B. Hu, 2007: A weak-constraint-based data assimilation scheme for estimating surface turbulent fluxes. *IEEE Geosci. Remote Sens. Lett.*, **4**, 649–653, https://doi.org/10.1109/LGRS.2007.904004.

Reichle, R. H., S. V. Kumar, S. P. P. Mahanama, R. D. Koster, and Q. Liu, 2010: Assimilation of satellite-derived skin temperature observations into land surface models. *J. Hydrometeor.*, **11**, 1103–1122, https://doi.org/10.1175/2010JHM1262.1.

Rodell, M., and Coauthors, 2004: The Global Land Data Assimilation System. *Bull. Amer. Meteor. Soc.*, **85**, 381–394, https://doi.org/10.1175/BAMS-85-3-381.

SAS, 2018a: SAS/STAT 15.1 user's guide: The NPAR1WAY procedure. SAS Institute Doc., 83 pp., https://support.sas.com/documentation/onlinedoc/stat/151/npar1way.pdf.

——, 2018b: SAS/STAT 15.1 user's guide: The TTEST procedure. SAS Institute Doc., 102 pp., https://support.sas.com/documentation/onlinedoc/stat/151/ttest.pdf.

——, 2018c: SAS/STAT 15.1 user's guide: The ANOVA procedure. SAS Institute Doc., 64 pp., https://support.sas.com/documentation/onlinedoc/stat/151/anova.pdf.

Schwingshackl, C., M. Hirschi, and S. I. Seneviratne, 2018: Global contributions of incoming radiation and land surface conditions to maximum near-surface air temperature variability and trend. *Geophys. Res. Lett.*, **45**, 5034–5044, https://doi.org/10.1029/2018GL077794.

Shiff, S., D. Helman, and I. M. Lensky, 2021: Worldwide continuous gap-filled MODIS land surface temperature dataset. *Sci. Data*, **8**, 74, https://doi.org/10.1038/s41597-021-00861-7.

Tomlinson, C. J., L. Chapman, J. E. Thornes, and C. Baker, 2011: Remote sensing land surface temperature for meteorology and climatology: A review. *Meteor. Appl.*, **18**, 296–306, https://doi.org/10.1002/met.287.

Trenberth, K. E., and Coauthors, 2007: Observations: Surface and atmospheric climate change. *Climate Change 2007: The Physical Science Basis*, S. Solomon et al., Eds., Cambridge University Press, 235–336.

Wan, Z., 2008: New refinements and validation of the MODIS land-surface temperature/emissivity products. *Remote Sens. Environ.*, **112**, 59–74, https://doi.org/10.1016/j.rse.2006.06.026.

——, 2013: Collection-6 MODIS land surface temperature products users' guide. ERI Doc., 35 pp., https://lpdaac.usgs.gov/documents/118/MOD11_User_Guide_V6.pdf.

——, Y. Zhang, Q. Zhang, and Z.-L. Li, 2002: Validation of the land-surface temperature products retrieved from *Terra* Moderate Resolution Imaging Spectroradiometer data. *Remote Sens. Environ.*, **83**, 163–180, https://doi.org/10.1016/S0034-4257(02)00093-7.

——, ——, ——, and ——, 2004: Quality assessment and validation of the MODIS global land surface temperature. *Int. J. Remote Sens.*, **25**, 261–274, https://doi.org/10.1080/0143116031000116417.

Wang, T., J. Shi, Y. Ma, L. Husi, E. Comyn-Platt, D. Ji, T. Zhao, and C. Xiong, 2019: Recovering land surface temperature

Brought to you by NOAA Central Library | Unauthenticated | Downloaded 07/19/23 03:29 PM UTC

under cloudy skies considering the solar-cloud-satellite geometry: Application to MODIS and Landsat-8 data. *J. Geophys. Res. Atmos.*, **124**, 3401–3416, https://doi.org/10.1029/2018JD028976.

Williamson, S. N., D. S. Hik, J. A. Gamon, J. L. Kavanaugh, and S. Koh, 2013: Evaluating cloud contamination in clear-sky MODIS *Terra* daytime land surface temperatures using ground-based meteorology station observations. *J. Climate*, **26**, 1551–1560, https://doi.org/10.1175/JCLI-D-12-00250.1.

WMO, 2016: The global observing system for climate: Implementation needs. GCOS Rep. GCOS-200, 342 pp., https://library.wmo.int/doc_num.php?explnum_id=3417.

Yan, Y., and Coauthors, 2020: Driving forces of land surface temperature anomalous changes in North America in 2002–2018. *Sci. Rep.*, **10**, 6931, https://doi.org/10.1038/s41598-020-63701-5.

Zeng, X., and A. Wang, 2012: What is monthly mean land surface air temperature? *Eos, Trans. Amer. Geophys. Union*, **93**, 156–156, https://doi.org/10.1029/2012EO150006.

Zhang, X., J. Pang, and L. Li, 2015: Estimation of land surface temperature under cloudy skies using combined diurnal solar radiation and surface temperature evolution. *Remote Sens.*, **7**, 905–921, https://doi.org/10.3390/rs70100905.

Zhang, Y., Y. Chen, J. Li, and X. Chen, 2020: A simple method for converting 1-km resolution daily clear-sky LST into real LST. *Remote Sens.*, **12**, 1641, https://doi.org/10.3390/rs12101641.

Zhang, Z., Y. Zhang, Y. Zhang, and J. M. Chen, 2020: Correcting clear-sky bias in gross primary production modeling from satellite solar-induced chlorophyll fluorescence data. *J. Geophys. Res. Biogeosci.*, **125**, e2020JG005822, https://doi.org/10.1029/2020JG005822.

Zhao, W., and S.-B. Duan, 2020: Reconstruction of daytime land surface temperatures under cloud-covered conditions using integrated MODIS/Terra land products and MSG geostationary satellite data. *Remote Sens. Environ.*, **247**, 111931, https://doi.org/10.1016/j.rse.2020.111931.

Brought to you by NOAA Central Library | Unauthenticated | Downloaded 07/19/23 03:29 PM UTC